metals

MDPI

Article

Selective Extraction of Lithium from Spent Lithium-Ion Manganese Oxide Battery System through Sulfating Roasting and Water-Leaching

Jeraldiny Becker *, Sebastian Will and Bernd Friedrich

IME Process Metallurgy and Metal Recycling, RWTH University, 52062 Aachen, Germany; sebastian.will@rwth-aachen.de (S.W.); bfriedrich@ime-aachen.de (B.F.)
* Correspondence: jbecker@ime-aachen.de

Abstract: Sulfating roasting tests were conducted with different agents to investigate lithium recovery from spent lithium-ion manganese oxide (LMO) batteries. In this study, $CaSO_4$ and $CaCO_3$ were used as reactants, and the optimal temperature, residence time, and molar fraction of $CaSO_4$ in a static reactor were determined. In the experiments, the temperature ranged between 620 and 720 °C, and the holding time was between 10 and 40 min. In addition, the molar fraction of $CaSO_4$ varied between 0 and 100%, with the rest being $CaCO_3$. The water leaching was fixed at a S/L ratio of 1/20 and heated to 60 °C for 1 h. The maximum Li yield achieved was 93.4% at 720 °C, 25 min, and a 0.5 molar fraction of $CaSO_4$, and virtually no Mn was present in the solution. Therefore, high selectivity for Mn—which is the major compound in the LMO black mass—was observed. Regarding statistical evaluation, temperature was the most influential parameter and, to a lesser extent, the molar fraction of $CaSO_4$. The product displayed a sintering effect, suggesting that the pyrolyzed black mass and reactive underwent a solid-solid reaction in the selected temperature range.

Keywords: LMO recycling; lithium recovery; sulfating roasting; water-leaching

check for updates

Citation: Becker, J.; Will, S.; Friedrich, B. Selective Extraction of Lithium from Spent Lithium-Ion Manganese Oxide Battery System through Sulfating Roasting and Water-Leaching. *Metals* **2023**, *13*, 1612. https://doi.org/10.3390/met13091612

Academic Editor: Ilhwan Park

Received: 15 August 2023
Revised: 11 September 2023
Accepted: 13 September 2023
Published: 18 September 2023

1. Introduction

The world is facing a severe climate crisis, and modern societies must reduce the greenhouse gas (GHG) concentration in the atmosphere to restrain this situation. The transportation sector is responsible for 16.2% of the yearly GHG emissions (2019) [1]. As a solution, the vehicle sector is getting electrified. To account for the demand for LiBs for this transformation, all around Europe, gigafactories are planned for the following years [2].

To produce these batteries, strategic raw materials are required. The list includes Li, Mn, graphite, and Ni in battery grade. According to the EU Commission, a strategic raw material is one of strategic importance, has forecasted demand growth, and is difficult to increase production [3].

To meet the demand for new batteries and prepare for the return of EoL (End of Life) batteries, a recycling route for LiBs must be proposed and established. Umicore, based in Belgium, has developed a pyrometallurgical recycling method for LiBs. The process employs a single-shaft furnace, with the charge comprising coke, slag former, and LiBs. The process uses the plastics to generate heat and produces an alloy comprising Cu, Co, and Ni. Al, Si, Ca, Fe, and Li are collected in the slag [4].

The disadvantages of this process are the high energy consumption and the loss of Li and other elements in the slag. A hydrometallurgical approach that can recover all cathodic metals with high recovery efficiency was introduced by Duesenfeld in Germany [5]. Their approach includes the leaching of the black mass from the LiBs, followed by several separation steps to extract all components of the black mass. Cu, Al, and Fe were recovered via precipitation. Ni, Co, and Mn were separated and recovered via solvent extraction. Finally, Li was recovered as Li_2CO_3 [6].

The main objective of this study is to selectively convert the Li in the black mass into a water-soluble compound. This means that after water leaching, only Li should be dissolved, which is also known as early-stage lithium recovery (ESLR). This can be achieved by roasting the black mass with reactants ($CaCO_3$ and $CaSO_4$).

2. Background

The fundamental principle of sulfating roasting is to selectively convert the desired metal into a sulfate that can dissolve in water. This is accomplished by incorporating various sulfate compounds during the roasting procedure. The objective is to ensure that impurities remain as insoluble compounds [7,8]. One of the benefits of utilizing sulfating roasting is that sulfates have high solubility in water, making the process convenient and eliminating the need for acid [9]. Sulfating roasting has been studied by some authors using different methods for recycling spent lithium batteries. In most cases, a solid additive is added to decompose during roasting so that the released SO_2 gas reacts with O_2 to produce SO_3, which reacts with the black mass. Some of the studied compounds are $(NH_4)_2SO_3$, $(NH_4)_2SO_4$, $NaHSO_4{\cdot}H_2O$, H_2SO_4, and Na_2SO_4 [8,10–14]. In other cases, a gas mixture of SO_2, O_2, and N_2 is used to control the partial pressures in the system and, therefore, to achieve selective sulfating roasting, according to predominance diagrams. Despite achieving a high lithium extraction (>90%) in the leaching step, other main elements such as Ni, Co, and Mn were also dissolved in the solution.

Wang et al. [10] use lithium-ion cobalt oxide batteries (LCO) from dismantled and disassembled batteries. The LCO is mixed with $NaHSO_4{\cdot}H_2O$. The sulfating roasting was conducted statically in a muffle furnace. The mixture was roasted in a sealed crucible at 600 °C for 30 min. Afterward, the roasted products are leached with deionized water and filtrated. Different ratios of LCO with additives were investigated. They discovered that the more additives they added, the more Co and less Li they found in the filter cake. The best result was a filter cake consisting of 72.56% Co and 0.53% Li. Shi et al. [7] used synthetic LCO powder for sulfating roasting. The experiments were performed in a static tube furnace with a gas inlet. The idea was to investigate how a gas mixture consisting of SO_2-O_2-Ar (10% SO_2 + 1% O_2) reacts with LCO. A reference experiment using only Ar was conducted. All other experiments were performed with the above mixture at different times. Afterward, the roasted products were leached with water for 60 min, at 25 °C with a S/L of 100 g/L. The LCO powder is converted through the process to a composition of Li_2SO_4, $Li_2Co(SO_4)_2$, and CoO. The best Li LE was 99.5% with a roasting time of 120 min. Moreover, 17.3% of Co was extracted. Lin et al. [11] performed their experiments with cathode material from spent, dismantled, and separated batteries. To burn organics, the material was baked at 500 °C for 300 min in a muffle furnace. Their additive H_2SO_4 was mixed with water and the NMC powder. The mixture was dried at 120 °C for 720 min. Afterward, the mixture was roasted in a tube furnace at 800 °C for 120 min. The roasted products were leached with water for 60 min at room temperature (RT) with a S/L of 200 g/L. Their best-attained Li LE was 96.92%, with all other elements being below 1%. Di et al. [12] performed static sulfating roasting in a tube furnace. They used NMC532, which was thermally treated at 500 °C for 60 min. The additive they used is Na_2SO_4 and was mixed with the NMC532. Afterward, the mixture was put into a crucible in a tube furnace. The roasted products were leached with water for 120 min at 80 °C with a S/L of 50 g/L. Their best Li LE was 85.43% with roasting parameters of 750 °C, 1:1 ratio, and 90 min. The LEs for Co, Mn, and Ni were below 0.5%. They found that the LE of Li increases with temperature until 750 °C. Adding more Na_2SO_4 above a ratio of 1:1 had no effect on the Li LE. Zhang et al. [13] used cathode powder from spent, dismantled, and separated batteries. The powder (NMC111) was treated in a muffle furnace at 400 °C for 60 min to burn organics. The NMC111 was mixed with $(NH4)_2SO_4$ and placed in a sealed crucible in a muffle furnace. Their investigation was about different roasting times, compositions, and temperatures. Afterward, the roasted products were leached with deionized water for 5–10 min at 25 °C. Their best Li LE was 98.31%, with other metals in the same range. The

roasting conditions for this LE were 400 °C, 1:3.5, and 20 min. Liu et al. [8] experimented with LMO powder from spent, dismantled, and separated batteries. To remove organics, the LMO was roasted in a muffle furnace at 600 °C for 600 min. The LMO was mixed with $NaHSO_4 \cdot H_2O$. The mixture was roasted in a sealed crucible placed in a muffle furnace. Afterward, the roasted products were leached with deionized water for 30 min at 60 °C with a S/L of 40 g/L. They found that the higher the quantity of additive, the higher the extraction rate. Their best conditions were 600 °C, 1:1.07, and 30 min. The resulting Li LE was 96.6% with an Mn LE of 9.7%.

The physicochemical properties of the sulfating roasting of spent lithium batteries with $CaSO_4$ and $CaCO_3$ have not been studied. Normally, it is expected that the agents decompose to allow a gas-solid reaction between the black mass and SO_3. However, the temperature must not exceed 750 °C, from which, according to preliminary experiments, Li extraction becomes poor, and beyond 850 °C, the material starts to melt. Furthermore, the melting temperature of Li_2CO_3 is 723 °C. Although the decomposition of CaSO4 occurs above 950 °C, solid-solid reactions can occur, allowing the transformation of Li compounds into Li_2SO_4 at lower temperatures. The major reactions that could occur in these mixtures at 620–720 °C are the solid-state exchange reactions of Li_2CO_3 with $CaSO_4$ and LiF with $CaCO_3$ or $CaSO_4$, listed in Table 1. Each reaction is provided with the respective ΔG°. The first three reactions and the last reaction show a negative ΔG°. All reactions, including Mn, display a positive ΔG°. This provides a basis for the selectivity of the process because MnO is not converted into the soluble $MnSO_4$ in the investigated temperature range.

Table 1. Reactions between active material, by-products, impurities, and reactants and their respective changes in Gibbs free energy *, grouped by element.

Element	Reaction	ΔG^0_{620} [kJ/mol]	ΔG^0_{720} [kJ/mol]
Li	$Li_2CO_3 + CaSO_4 \rightarrow Li_2SO_4 + CaCO_3$	−2.95	−7.09
	$2\ LiF + CaSO_4 \rightarrow Li_2SO_4 + CaF_2$	−13.11	−18.31
	$2\ LiF + CaCO_3 \rightarrow Li_2CO_3 + CaF_2$	−10.16	−11.22
Mn	$MnO + CaSO_4 \rightarrow MnSO_4 + CaO$	129.93	130.94
	$2MnO + CaCO_3 \rightarrow Mn_2CO_3 + CaO$	85.13	87.74
C	$CaSO_4 + 2\ C \rightarrow CaS + 2\ CO_2\ (g)$	−152.11	−187.25

* Calculated with Factsage database FactPS.

Other possible reactions, such as the reactions of $LiMnO_2$ with $CaCO_3$ and $CaSO_4$, are listed below. With $CaSO_4$, there are two possible reactions, depending on the amount of CaSO4.

$$4\ LiMnO_2 + 2\ CaCO_3 = 2\ Li_2CO_3 + 4\ MnO + 2\ CaO + O_2\ (g)$$

$$4\ LiMnO_2 + 2\ CaSO_4 = 2\ Li_2SO_4 + 4\ MnO + 2\ CaO + O_2\ (g)$$

$$4\ LiMnO_2 + 6\ CaSO_4 = 2\ Li_2SO_4 + 4\ MnS + 6\ CaO + 9\ O_2\ (g)$$

The sulfating roasting focused on the transformation into Li compounds with high solubility for the subsequent neutral leaching. The water solubilities of various Li compounds at different temperatures are listed in Table 2.

Table 2. Solubility of different lithium compounds in water [15].

Temp.	Solubility in g/100 mL			
	LiOH	Li_2CO_3	Li_2SO_4	LiF
20 °C	11.0	1.33	25.6	0.131
60 °C	12.7	0.99	24.5	0.134
100 °C	16.1	0.72	23.6	0.134

Table 3 summarizes the conditions and results of other studies using the same principle. For solid reactants, the temperature used depends largely on the decomposition temperature. As a result, in most cases, Li extraction is high. However, the co-dissolution of other metals ranges from unavailability to low or high values.

Table 3. Summary of conditions for lithium extraction using sulfating roasting found in literature.

Input Material	Roasting Reactants	Roasting			Leaching Efficiency [%]				Ref.
		Temp. [°C]	Time [min]	Mass Ratio * (or Flow Rate)	Li	Co	Ni	Mn	
Spent LCO	$NaHSO_4 \cdot H_2O$	600	30	1:1.4	N/A	N/A	N/A	N/A	Wang 2018 [10]
Synthetic LCO	10% SO_2 + 1% O_2	700	120	400 mL/min	99.5	N/A	N/A	N/A	Shi 2019 [7]
Spent LiB	H_2SO_4	800	120	2:1	96.92	0.33	0.15	1.04	Lin 2020 [11]
Spent LiB	Na_2SO_4	750	90	1:1	85.43	0	0	0	Di 2020 [12]
Spent NMC 111	$(NH_4)_2SO_4$	400	20	1:3.5	98.31	97.32	96.29	97.30	Zhang 2021 [13]
Spent LMO	$NaHSO_4 \cdot H_2O$	600	30	1:1.07	96.6	N/A	N/A	9.7	Liu 2022 [8]
Spent NMC	$(NH_4)_2SO_3$	550	150	1:2 **	88	<0.03	<0.03	<0.03	Cao 2022 [15]
Spent LCO	10% SO_2 + 10% O_2	850	60	500 mL/min	99.51	61.21	22.99	68.36	Biswas 2023 [9]

* Ratio feedstock:reactant; ** molar ratio.

3. Materials and Methods

The black mass received from the company Promesa was pyrolyzed at 600 °C for 1 h under an N_2 atmosphere. The pyrolyzed material was then sieved at 125 µm, separating a large amount of Al and Cu in the coarser fraction. Chemical analysis of the <125 µm fraction is shown in Table 4.

Table 4. Chemical composition of <125 µm fraction of the pyrolyzed black mass.

Elem.	Al	Co	Cu	Fe	Li	Mn	Ni	F	S	C
wt.%	0.45	0.27	0.75	0.66	4.34	46.5	0.61	2.39	0.35	12.4

The chemical composition reveals that it is an LMO battery owing to its high Mn content and much lower Co and Ni contents. Figure 1 shows the phases found in the pyrolyzed black mass by XRD.

During pyrolysis, decomposition reactions of the LMO battery occur, as do reactions between the CO_2 (g) from the decomposition of the organics and the black mass. Some possible reactions are as follows:

$$12\ LiMn_2O_4 \rightarrow 6\ LiMnO_2 + Mn_3O_4 + 5\ O_2\ (g)$$

$$4\ LiMnO_2 + 2\ CO_2\ (g) = 2\ Li_2CO_3 + 4\ MnO + O_2\ (g)$$

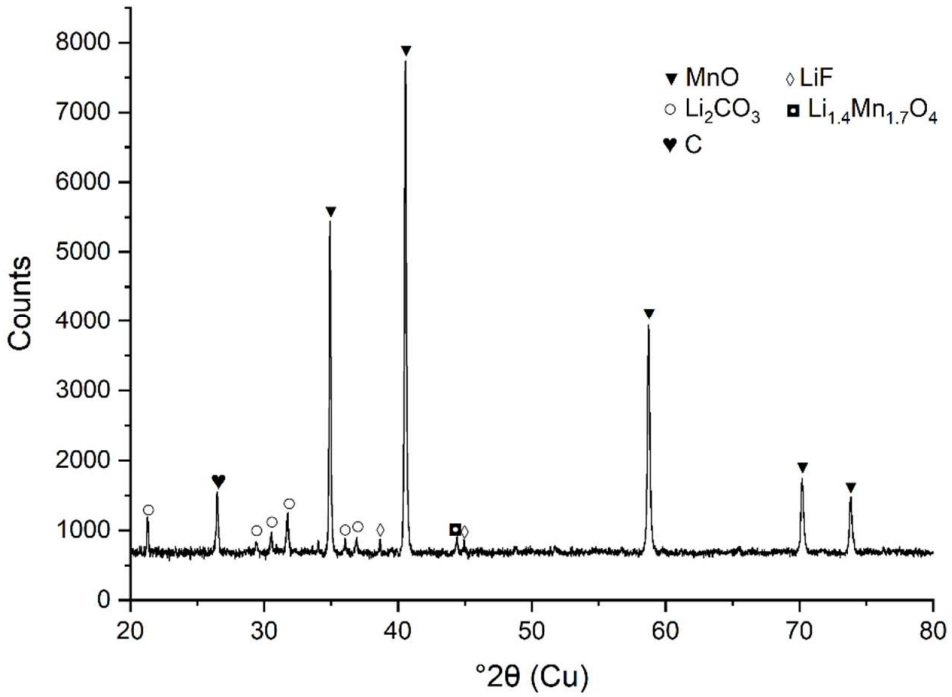

Figure 1. Diffractogram of pyrolyzed black mass (<125 µm fraction).

The pyrolyzed black mass was mixed with the reactants at a given mass ratio for the trial. Both reactants, $CaCO_3$ and $CaSO_4$, are in chemical grade from Sigma-Aldrich. $CaSO_4$ has a particle size of 44 µm and a purity of 99% (Sigma Aldrich SID 329752446, Darmstadt, Germany). $CaCO_3$ has a particle size of 44 µm and a purity of >99.0% (Sigma Aldrich SID 329752519, Darmstadt, Germany).

Two types of furnaces were used to adjust the range of the main parameters of the sulfating roasting. A rotary and static oven at a lab scale were employed to determine the best performance for the transformation of lithium into a water-soluble compound. An optimal performance was achieved using a static furnace. The permanent friction of the particles in the rotary kiln hinders the ongoing reactions and permanently breaks the interparticle contact. During roasting, these mixtures can only undergo solid-state reactions based on the interdiffusion of cations between the particles of different components. This type of reaction is usually favored by a fine particle size (smaller diffusion distance) and a high temperature (higher coefficient of diffusion) [16].

Furthermore, the temperature in the rotary kiln cannot be measured inside the furnace. Therefore, the temperature was lower than the set point, and the temperature delta remained unknown. For the static experiments, the temperature of the sample was measured. In addition, the mass balance can be carried out more easily in comparison with a rotary kiln, where some material remains attached to the wall. Once the reactor was selected, the input materials were mixed and placed in an alumina crucible. Thermal treatment was conducted, followed by milling of the sample. Subsequently, the sample was leached with deionized water and filtered. Samples of the filter cake and leach solution after filtration were analyzed.

All steps accompanying the roasting, i.e., thermal pre-treatment, are shown in Figure 2.

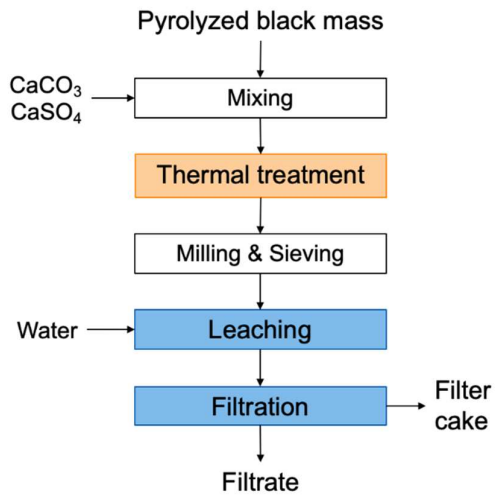

Figure 2. Schematic of the experimental procedure.

3.1. DoE

To obtain information on the effects of the roasting parameters on the leaching efficiency, a design of the experiment was planned. The face-centered design (CCF), which is part of the central composite design (CCD), created a surface response with 15 experiments. A full factorial design would involve 27 experiments; however, using a CCF design would reduce the number of experiments to 15, as shown in Table 5 [17].

Table 5. Levels of the factors of DoE used in the sulfating roasting process.

Factors	Levels		
	Low	Center	High
	(−1)	(0)	(+1)
Temperature	620	670	720
Holding time	10	25	40
Molar Fraction $CaSO_4$	0	0.5	1

The available literature indicates that the optimal temperature range for the experiment is 600–800 °C. Therefore, this temperature range was established as the appropriate range for the experiments. The CCD requires setting factors outside this temperature range. In addition, the holding time could be suggested to be negative, which could not be achieved. To ensure that the temperature remains within the recommended range and that the holding time is achievable, a decision was made to utilize the CCF. Based on the observation that a high ratio of reactants led to better Li LE, all the main trials were performed with a high ratio of reactants, using 15 g of black mass and 30 g of reactants. The molar fraction of $CaSO_4$ was varied between 0, 0.5, and 1 to determine the composition of the reactants. These levels corresponded to 30 g of $CaCO_3$ for level 0, 17.29 g of $CaSO_4$ + 12.71 g of $CaCO_3$ for level 0.5, and 30 g of $CaSO_4$ for level 1, resulting in a change in the ratio of $CaCO_3$ to $CaSO_4$.

3.2. Experimental Procedure

For the main trials, the input material (15 g black mass plus 30 g reactants) was weighed and mixed before each trial. All three ingredients were weighed in a plastic bowl and mixed with a spatula. Mixing was performed manually until no recognizable parts of the agglomerations remained and a homogeneous gray material was obtained. The material was placed into an alumina crucible. The crucible was placed in a reactor in a Thermo-Star furnace. The crucible was weighed empty before roasting and full/empty after roasting to examine mass losses. Figure 3 displays the setup of the main trials. The crucible is in the middle of the reactor, with a thermocouple in the sample. The reactor

stands between the heating elements of the Thermo-Star furnace. The lid of the reactor is airtight. Two connections are at the top for the gas in-/outlet. Afterward, the furnace is heated up with a ramp of 300 °C per hour until the holding temperature (±5 °C) is reached. After the temperature is reached, the holding time starts. The furnace is left to cool down when the holding time is over. While cooling down, the reactor is flushed with 1.5 L/min of N2. The materials were obtained from the cooled-down crucible, milled, and then sieved. The material was ground and sieved until less than 1 g of the material >125 µm remained as residue. The <125 µm fraction was used for leaching. All trials were conducted using the same parameters. The material was leached for 60 min at 60 °C at a S/L ratio of 50 g/L.

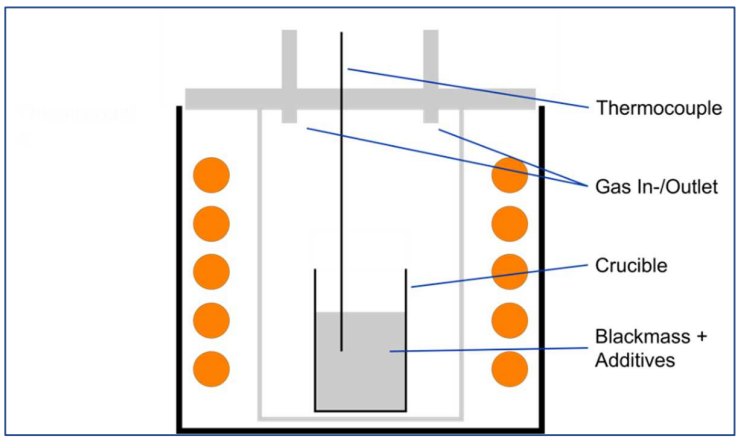

Figure 3. Setup of roasting step.

3.3. Calculation of Leaching Efficiency and Selectivity

Equation (1) determines Li leaching efficiency by comparing the amount of Li in filtrate with the sum of Li in filtrate and filter cake fraction. This is to mitigate the effects of non-uniformity in the black mass and the potential loss of mass during thermal treatment.

$$LE = \frac{C_F \times V}{C_F \times V + C_{FC} \times m_{FC}} \times 100 \quad (1)$$

where C_F is the concentration of element in the filtrate (g/L), C_{FC} is the concentration of element in the filter cake (%), V is the volume of the filtrate (L), and m_{FC} is the mass of the filter cake (g).

To evaluate the efficiency of the separation of metals, the selectivity factor (SF) was considered. The SF is the deviation of the concentration of Li in the filtrate divided by the concentration of another metal in the filtrate, as shown in Equation (2) [18].

$$SF = \frac{C_{Li}}{C_M} \quad (2)$$

with C_{Li} being the concentration of Li in the filtrate (g/L) and C_M being the concentration of another element in the filtrate (g/L).

4. Results and Discussion

4.1. Extraction of Lithium

Results obtained from the leaching tests are shown in Table 6, where the extraction percentage for each element was averaged with its respective deviation.

Table 6. Leaching efficiency for different metals of LMO via sulfating roasting and water leaching.

Test Order	Factors			Responses—Leaching Efficiency (%)					
	Temp. [°C]	Holding Time [min]	Molar Fraction $CaSO_4$	Li	Al	Cu	Co	Mn	Ni
1	720	40	0	90.2	4.4	3.2	5.4	0.1	3.1
2	670	25	0	89.6	4.3	3.1	5.1	0.1	2.9
3	670	40	0.5	92.2	4.5	3.4	7.3	0.1	3.7
4	620	10	1	90.2	0.3	3.1	4.8	0.1	2.6
5	620	25	0.5	90.5	4.7	2.9	4.6	0.1	2.5
6	670	25	1	90.6	0.3	3.1	4.5	0.1	2.6
7	720	10	0	92.0	4.4	3.8	10.3	0.1	5.4
8	720	10	1	92.2	4.7	3.6	8.7	0.1	4.2
9	670	25	0.5	92.7	4.9	3.8	9.0	0.1	4.4
10	720	40	1	93.0	4.7	3.5	8.7	0.1	4.1
11	620	40	0	88.9	0.3	2.7	4.2	0.1	2.3
12	620	40	1	90.6	4.7	3.3	5.6	0.1	3.4
13	620	10	0	89.0	4.3	3.1	5.6	0.1	3.3
14	720	25	0.5	93.4	4.7	3.6	8.6	0.1	4.2
15	670	10	0.5	90.5	4.7	3.1	4.7	0.1	2.5

It is noteworthy that the results of the chemical analysis for Al, Co, Cu, Mn, and Ni were <1 mg/L in the solutions; for calculation purposes, a value of 0.5 mg/L was considered.

For all trials, Li extraction yielded above 88%. Furthermore, Mn coextraction does not even reach 0.1% in all cases, a standout result when considering its high quantity in the black mass (46.5%).

4.2. Comparison of the Influence of $CaSO_4$ and $CaCO_3$ on Other Elements

When the results are grouped by the molar fraction, the following effects on the fluoride ions in the solution are evident: As shown in Figure 4, Li was co-distributed with F in the filtrate when only $CaCO_3$ was present. In comparison, when $CaSO_4$ was used, S and Ca were present; however, F decreased significantly. This leads to the assumption that $CaSO_4$ reacts with LiF and fixes it as CaF_2, which is an insoluble compound. When using a sample with both $CaCO_3$ and $CaSO_4$, dissolution of S and Ca was also observed, whereas dissolution of Al, Cu, Co, Mn, Ni, Fe, and P was minimal in all cases.

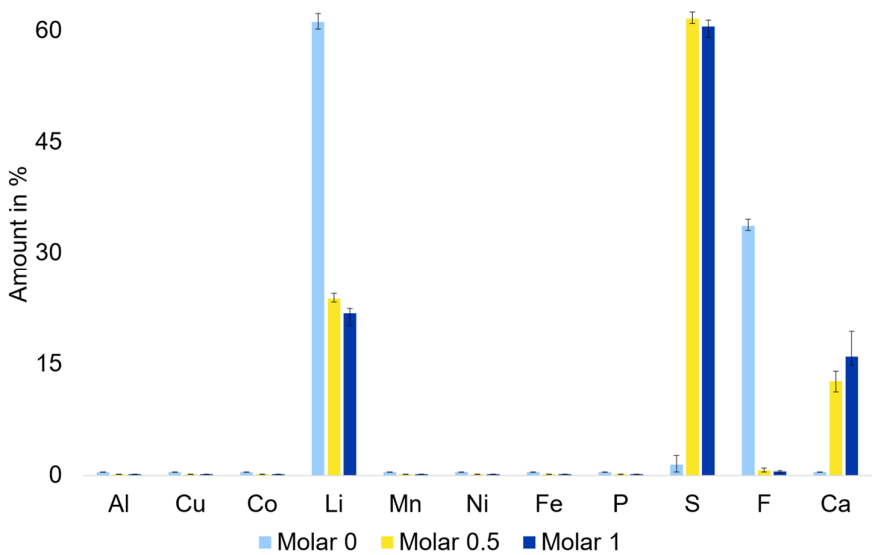

Figure 4. Average amount in % of each element in all trials, sorted by Molar Fraction, in the filtrate.

The average number of elements in the filter cake is shown in Figure 5. The filter cake contained high levels of Mn, C, and elements derived from the reactants such as Ca and S. When $CaSO_4$ is used, F is fixed in this phase. In addition, Al and P were present in the filter cake.

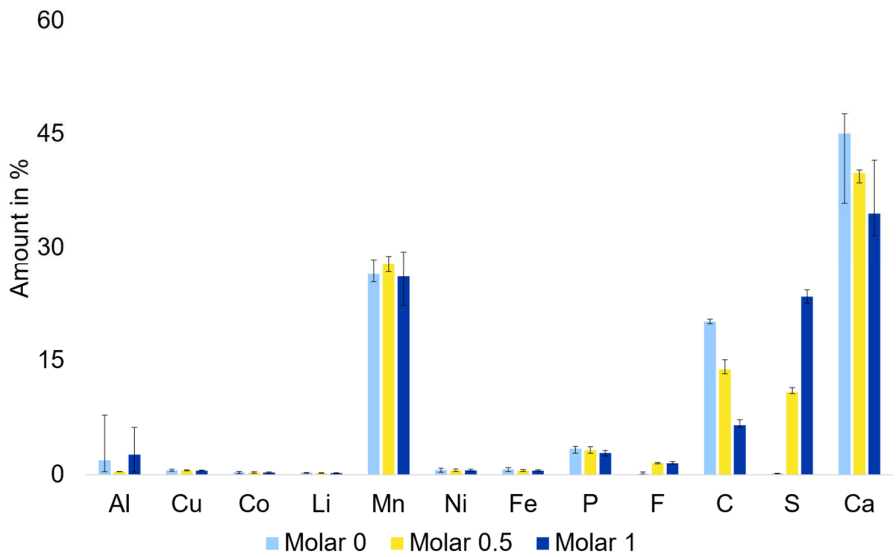

Figure 5. Average amount in % of each element in all trials, sorted by Molar Fraction, in the filter cake.

4.3. Statistical Analysis—Effects and Interactions

Statistical analysis demonstrates the importance of the individual variables in the model, including the main effects, interactions, and parameter optimization.

The Pareto chart is a valuable tool for examining the statistically significant terms and their relative magnitudes within the model. Figure 6 presents the Pareto chart corresponding to the model, with Li LE as the response variable, where any bar surpassing the red-dotted line indicates statistical significance with a *p*-value less than 0.05. Notably, temperature, molar fraction, and the squared term of the molar fraction emerged as three statistically significant terms. Among these terms, temperature exerted the most substantial influence on the model. The molar fraction and squared molar fraction exhibited comparable impact magnitudes, albeit slightly lower than temperature. This Pareto analysis offers valuable insight into the relative significance of each term within the model.

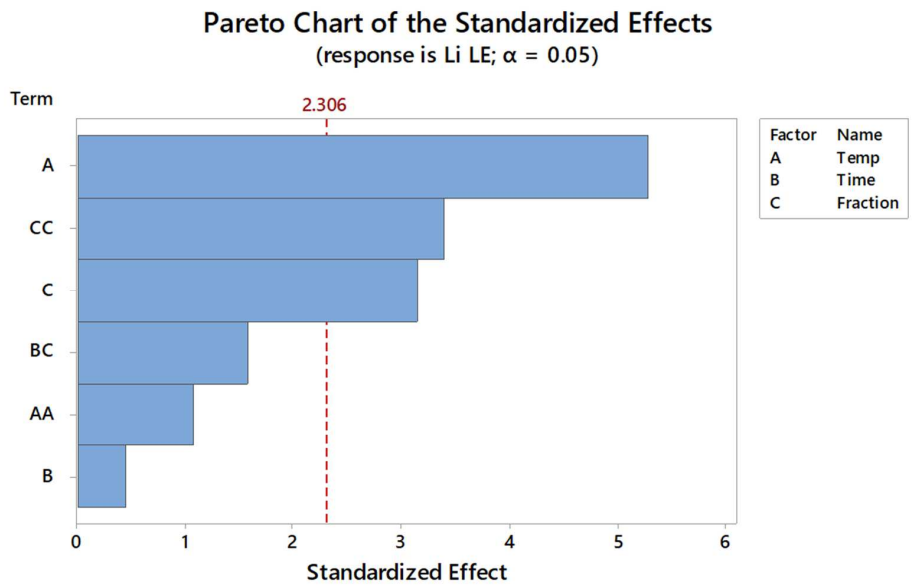

Figure 6. Pareto distribution.

The main effects quantify the contribution of each factor to the mean response of Li LE. Figure 7 illustrates the main effect plots. An increase in the temperature was observed to positively influence the response. In contrast, the impact of the holding time on the response is relatively minor, as depicted by the small bar in Figure 6. The molar fraction exhibited a parabolic effect on the response. Specifically, the response was lowest when only $CaCO_3$ was present, whereas the highest response was achieved when a mixture of both reactants was used.

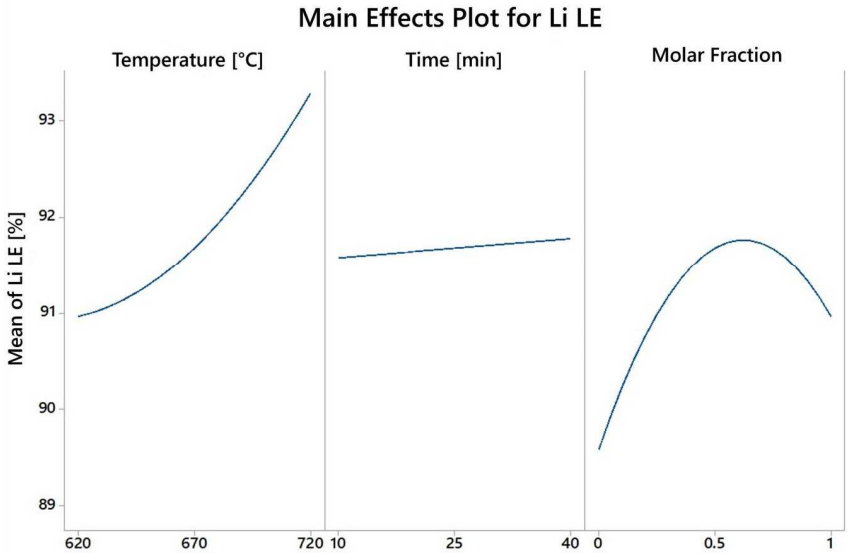

Figure 7. Main effects for lithium extraction through sulfating roasting.

Interaction plots revealed the relationships between different factors. In the model, the interaction between time and molar fraction, labeled Time·Fraction, remains significant. Figure 8 depicts the interaction plot between time and molar fraction. It can be observed that the impact of the molar fraction becomes more pronounced with longer holding times. Specifically, when only $CaSO_4$ was present, time had a positive effect on mean Li LE. Conversely, when only $CaCO_3$ is used, the effect is negative. However, when a molar fraction of 0.5 is employed, the effect becomes negligible.

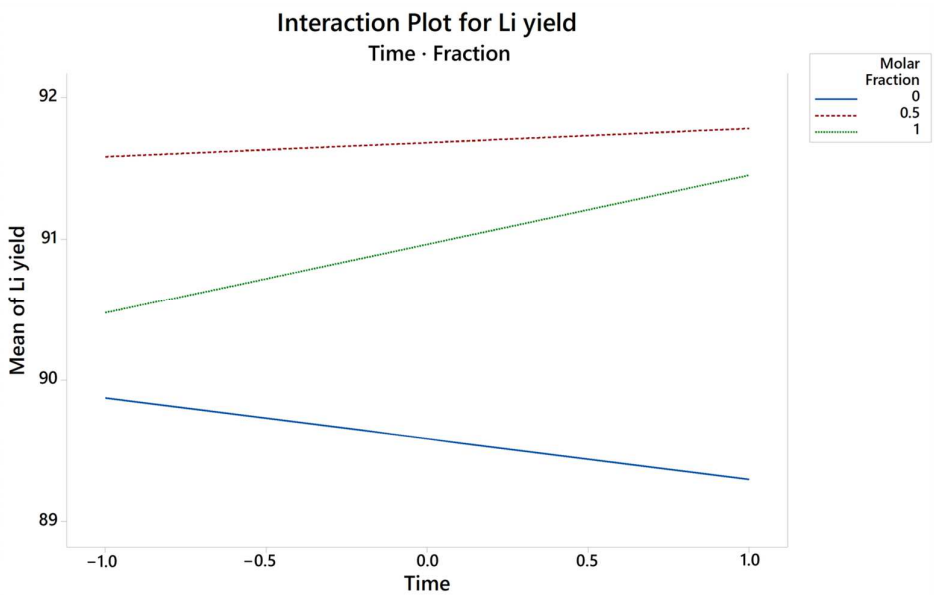

Figure 8. Interaction plot of the factors time and molar fraction with Li LE as a response.

Furthermore, by maximizing the response and eliminating some factors and interactions, it is possible to reach a maximum value of 93.6% for Li extraction for a given S/L value, which is the determining parameter, together with the particle size, to achieve superior extraction. However, in this study, we limited ourselves to a S/L ratio of 1/20, which would be a limiting value to scale the process industrially.

4.4. Selectivity

The selectivity factor (SF) represents the leached amount of an element relative to the leached amount of Li. Thus, it determines the purity of the resulting aqueous solution [19]. Higher SF values indicate greater selectivity. Regarding LiB recycling, some authors state that their processes are selective but do not quantify it [20–24]. Across all the main trials, the SF values for Al, Cu, Co, Mn, Ni, Fe, and P fell within the range of 128 to 142. The SF values for S, F, and Ca are listed in Table 7 and sorted by molar fraction. For molar fractions of 0.5 and 1, the SF values for S ranged from 34 to 40, while the SF values for F ranged from 24 to 65. The SF values for Ca in these molar fractions are very low, ranging from 1 to 2. At a molar fraction of 0, the SF value for F is low (approximately 1.8). Conversely, the SF value for Ca in molar fraction 0 ranged from 129 to 138, which was similar to the SF values of other impurities across all molar fractions. As no S was added to molar fraction 0, the SF value for S was high.

Table 7. SF for each main trial for elements S, F, and Ca sorted by molar fraction.

Trial	Molar Fraction $CaSO_4$	Li/S	Li/F	Li/Ca
4	1	36.2	35.6	1.5
6	1	35.5	43.3	1.4
8	1	37.1	43.9	1.8
10	1	34.1	65.0	1.0
12	1	36.8	34.8	1.5
3	0.5	38.3	40.8	1.8
5	0.5	38.3	24.2	2.1
9	0.5	39.6	36.3	2.1
14	0.5	38.2	48.3	1.7
15	0.5	38.0	31.8	1.8
1	0	6699.3	1.9	138.0
2	0	13,740.0	1.9	137.4
7	0	5684.2	1.8	129.6
11	0	2794.0	1.8	130.2
13	0	2251.7	1.8	136.0

5. Discussion

5.1. Possible Reactions and Mechanisms

The sintering effect revealed a reaction on the surface of the particles. A maximum mass loss of only 5% was observed. As previously presented, solid-state reactions occur, allowing transformation to Li_2SO_4. Li-Mn oxides can react with both $CaCO_3$ and $CaSO_4$ to form Li_2CO_3 and Li_2SO_4, respectively.

The XRD patterns for two experiments after roasting and after leaching are shown in Figures 9 and 10. Equimolar amounts of $CaSO_4$ and $CaCO_3$ were used in these experiments. Both agents remained unreacted, allowing the possibility of decreasing their quantity in further studies. In both cases, Li_2CO_3 was not identified, indicating the transformation of Li_2CO_3 to Li_2SO_4. Furthermore, when $CaSO_4$ is used, MnS can be produced in parallel at both temperatures and is only identified after leaching. Furthermore, C was not detected in the diffractogram before leaching because its share was below the 5 wt.% required by the software HighScore (version 4.9) to be identified. After leaching, Li_2SO_4 was completely dissolved, as were, to some extent, $CaSO_4$ and $CaCO_3$, which are slightly soluble in water. The main difference between the two experiments was the type of Mn oxide detected, although their oxidation states were similar.

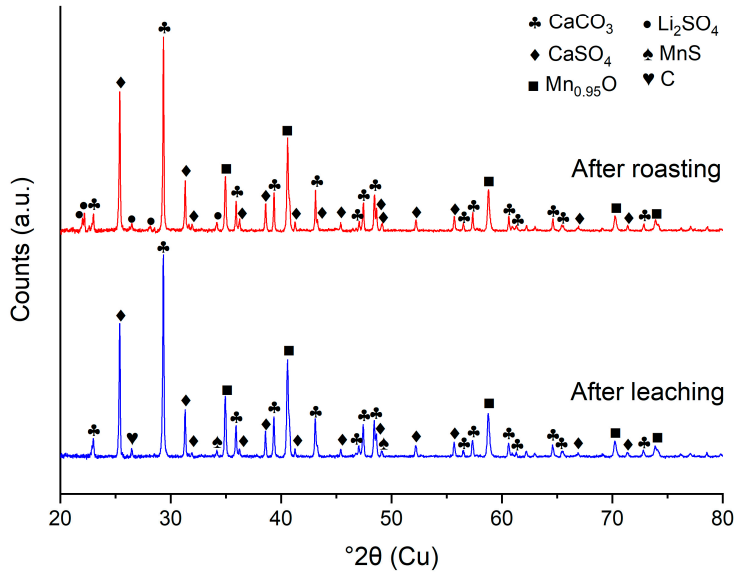

Figure 9. XRD analysis for experiment ST9 after roasting and after leaching. ST9 corresponds to a mixture of $CaCO_3$:$CaSO_4$ =1:1 at 670 °C.

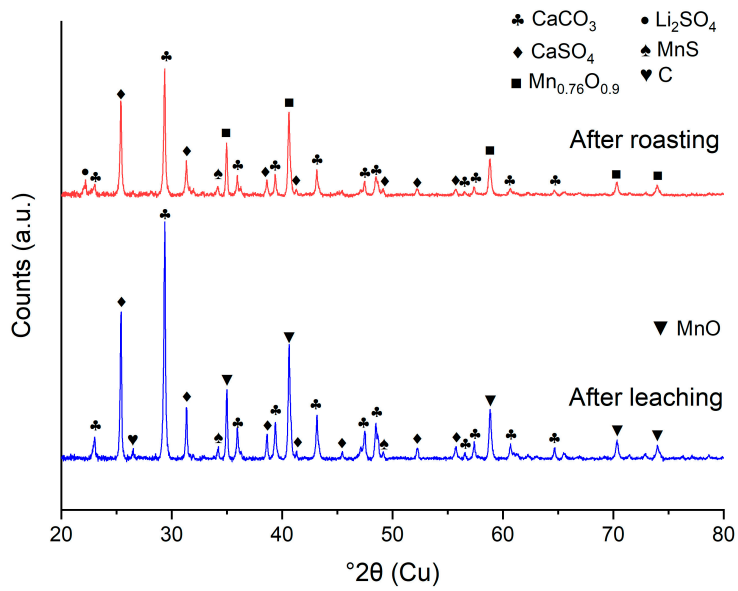

Figure 10. XRD analysis for experiment ST14 after roasting and after leaching. ST14 corresponds to a mixture of $CaCO_3$:$CaSO_4$ = 1:1 at 720 °C.

As $LiMn_2O_4$ cannot be completely decomposed by pyrolysis and some Li-Mn oxides are still present in the pyrolyzed black mass, not all Li can be recovered by water leaching after pyrolysis. $CaCO_3$ also served to recover Li with a high yield, indicating that a S/L ratio of 1/20 was sufficient to dissolve Li_2CO_3. Therefore, when $CaSO_4$ is used, the S/L ratio can be minimized owing to the solubility of the product. Therefore, the parameters can be optimized, and further studies on the leaching step are necessary.

5.2. Valorization of the Leached Residue

To obtain the remaining material from the leached residue, we recommend two methods. One method involves acid leaching to dissolve the components. Mn is regained by precipitation or solvent extraction as a salt. The remaining liquid is evaporated to obtain Ca as salt. On the other hand, carbothermic reduction can be performed with the residue to regain Mn as a metal.

6. Conclusions

A high Li leaching efficiency (LE) with a maximum value of 93.4% was achieved via sulfating roasting and water leaching. Statistical analysis revealed that the Li LE is dependent on the temperature as well as the quantity and mixture of reactants (expressed as the Molar Fraction of $CaSO_4$). Within the investigated temperature range, higher temperatures were found to be optimal for maximizing Li recovery. The combination of $CaSO_4$ and $CaCO_3$ resulted in the highest Li leaching efficiency. Based on the optimized parameter setup proposed by Minitab (version 17), the ideal conditions for achieving the highest Li LE are a temperature of 720 °C, a holding time of 40 min, and a mixture of 22.51 g $CaSO_4$ and 7.49 g $CaCO_3$.

The selectivity of the process was influenced by the quantity and mixture of reactants (Molar Fraction of $CaSO_4$). Notably, impurities such as S, F, and Ca were observed for Molar Fractions of 0.5 and 1, while only F impurities were present for Molar Fraction 0. In contrast, other elements remained in the filter cake and did not dissolve during leaching. The highest purity was achieved when using only $CaCO_3$ as the additive. Although theoretically a higher proportion of water is needed to dissolve all LiF, a yield above 85% was achieved in all experiments. The Mn leaching efficiency was approximately 0.1% for all cases.

Furthermore, Li was successfully recovered in the absence of $CaSO_4$. $CaCO_3$ also proves to be an alternative to thermally treating the black mass after pyrolysis.

Based on observations, such as sintering of the material and minimal mass loss, a solid-state reaction drives this process according to the presented reactions.

Author Contributions: Conceptualization, B.F.; Methodology, J.B.; Software, J.B. and S.W.; Formal analysis, S.W.; Investigation, J.B. and S.W.; Resources, B.F.; Writing—original draft, J.B. and S.W.; Writing—review and editing, J.B.; Visualization, S.W.; Supervision, J.B. and B.F.; Project administration, J.B.; Funding acquisition, B.F. All authors have read and agreed to the published version of the manuscript.

Funding: This research was funded by German Federal Environmental Foundation (DBU) grant number 35845/02.

Data Availability Statement: Data is contained within the article. The data presented in this study is available in the master thesis: "Will, S. (2023). Study of lithium recovery from spent LiBs based on sulfating roasting and water leaching. Rheinisch-Westfälische Technische Hochschule Aachen, Germany.", which can be provided upon request.

Conflicts of Interest: The authors declare no conflict of interest.

References

1. Ritchie, H.; Roser, M.; Rosado, P. CO_2 and Greenhouse Gas Emissions. Our World Data. 2020. Available online: https://ourworldindata.org/emissions-by-sector (accessed on 21 January 2023).
2. Zenn, R. Li-on Battery Gigafactories in Europe. OROVEL. Available online: https://www.orovel.net/insights/li-on-battery-gigafactories-in-europe-january-2021 (accessed on 14 October 2022).
3. Directorate-General for Internal Market, Industry, Entrepreneurship and SMEs. Proposal for a Regulation of the European Parliament and of the Council Establishing a Framework for Ensuring a Secure and Sustainable Supply of Critical Raw Mate-rials and Amending Regulations (EU) 168/2013, (EU) 2018/858, 2018/1724 and (EU) 2019/1020. European Commission, Brussels. 2023. Available online: https://single-market-economy.ec.europa.eu/publications/european-critical-raw-materials-act_en#details (accessed on 4 July 2023).
4. Cheret, D.; Santen, S. Battery Recycling. U.S. Patent US20050235775A1, 27 October 2005. Available online: https://patents.google.com/patent/US20050235775A1/ (accessed on 30 October 2022).
5. Mossali, E.; Picone, N.; Gentilini, L.; Rodrìguez, O.; Pérez, J.M.; Colledani, M. Lithium-ion batteries towards circular economy: A literature review of opportunities and issues of recycling treatments. *J. Environ. Manag.* **2020**, *264*, 110500. [CrossRef] [PubMed]
6. Christian, H.; Tobias, E.; Lisa, B. Method for Recycling Lithium Batteries. U.S. Patent WO2021018372A1, 4 February 2021. Available online: https://patents.google.com/patent/WO2021018372A1 (accessed on 2 November 2022).
7. Shi, J.; Peng, C.; Chen, M.; Li, Y.; Eric, H.; Klemettinen, L.; Lundström, M.; Taskinen, P.; Jokilaakso, A. Sulfation Roasting Mechanism for Spent Lithium-Ion Battery Metal Oxides Under SO_2-O_2-Ar Atmosphere. *JOM* **2019**, *71*, 4473–4482. [CrossRef]
8. Liu, Z.; Chen, H.; Wang, D.; Zhou, X.; Hu, P. Metal Recovery from Spent $LiMn_2O_4$ Cathode Material Based on Sulfating Roasting with $NaHSO_4 \cdot H_2O$ and Water Leaching. *J. Sustain. Metall.* **2022**, *8*, 684–699. [CrossRef]

9. Biswas, J.; Ulmala, S.; Wan, X.; Partinen, J.; Lundström, M.; Jokilaakso, A. Selective Sulfation Roasting for Cobalt and Lithium Extraction from Industrial LCO-Rich Spent Black Mass. *Metals* **2023**, *13*, 358. [CrossRef]
10. Wang, D.; Zhang, X.; Chen, H.; Sun, J. Separation of Li and Co from the active mass of spent Li-ion batteries by selective sulfating roasting with sodium bisulfate and water leaching. *Miner. Eng.* **2018**, *126*, 28–35. [CrossRef]
11. Lin, J.; Li, L.; Fan, E.; Liu, C.; Zhang, X.; Cao, H.; Sun, Z.; Chen, R. Conversion Mechanisms of Selective Extraction of Lithium from Spent Lithium-Ion Batteries by Sulfation Roasting. *ACS Appl. Mater. Interfaces* **2020**, *12*, 18482–18489. [CrossRef] [PubMed]
12. Di, C.; Yongming, C.; Yan, X.; Cong, C.; Yafei, J.; Fang, H. Selective Recovery of Lithium from Ternary Spent Lithium-Ion Batteries Using Sulfate Roasting-Water Leaching Process. In *Energy Technology 2020: Recycling, Carbon Dioxide Management, and other Technologies*; Chen, X., Zhong, Y., Zhang, L., Howarter, J.A., Baba, A.A., Wang, C., Sun, Z., Zhang, M., Olivetti, E., Luo, A., et al., Eds.; The Minerals, Metals & Materials Series; Springer International Publishing: Cham, Switzerland, 2020; pp. 387–395. [CrossRef]
13. Zhang, X.; Cai, L.; Fan, E.; Lin, J.; Wu, F.; Chen, R.; Li, L. Recovery valuable metals from spent lithium-ion batteries via a low-temperature roasting approach: Thermodynamics and conversion mechanism. *J. Hazard. Mater. Adv.* **2021**, *1*, 100003. [CrossRef]
14. Cao, N.; Zhang, Y.; Chen, L.; Jia, Y.; Huang, Y. Priority recovery of lithium and effective leaching of nickel and cobalt from spent lithium-ion battery. *Trans. Nonferrous Met. Soc. China* **2022**, *32*, 1677–1690. [CrossRef]
15. Haynes, W.M. *CRC Handbook of Chemistry and Physics*; CRC Press Taylor & Francis Group: Boca Raton, FL, USA, 2017; pp. 5–170.
16. Lemoisson, F.; Froyen, L. 12—Understanding and improving powder metallurgical processes. In *Fundamentals of Metallurgy*; Seetharaman, S., Ed.; Woodhead Publishing Series in Metals and Surface Engineering; Woodhead Publishing: Cambridge, UK, 2005; pp. 471–502. [CrossRef]
17. Siebertz, K.; van Bebber, D.; Hochkirchen, T. *Statistische Versuchsplanung*; Springer: Berlin/Heidelberg, Germany, 2017. [CrossRef]
18. Prasetyo, E.; Anderson, C.; Nurjaman, F.; Al Muttaqii, M.; Handoko, A.S.; Bahfie, F.; Mufakhir, F.R. Monosodium Glutamate as Selective Lixiviant for Alkaline Leaching of Zinc and Copper from Electric Arc Furnace Dust. *Metals* **2020**, *10*, 644. [CrossRef]
19. Smit, D.S. Chapter 2: Literature Survey. Available online: https://repository.nwu.ac.za/bitstream/handle/10394/9626/Smit_DS_Chapter_2.pdf?sequence=3&isAllowed=y (accessed on 18 January 2023).
20. Xiao, J.; Niu, B.; Xu, Z. Highly efficient selective recovery of lithium from spent lithium-ion batteries by thermal reduction with cheap ammonia reagent. *J. Hazard. Mater.* **2021**, *418*, 126319. [CrossRef] [PubMed]
21. Zhou, M.; Li, B.; Li, J.; Xu, Z. Pyrometallurgical Technology in the Recycling of a Spent Lithium Ion Battery: Evolution and the Challenge. *ACS EST Eng.* **2021**, *1*, 1369–1382. [CrossRef]
22. Yang, C.; Zhang, J.; Cao, Z.; Jing, Q.; Chen, Y.; Wang, C. Sustainable and Facile Process for Lithium Recovery from Spent $LiNi_xCo_yMn_zO_2$ Cathode Materials via Selective Sulfation with Ammonium Sulfate. *ACS Sustain. Chem. Eng.* **2020**, *8*, 15732–15739. [CrossRef]
23. Higuchi, A.; Ankei, N.; Nishihama, S.; Yoshizuka, K. Selective Recovery of Lithium from Cathode Materials of Spent Lithium Ion Battery. *JOM* **2016**, *68*, 2624–2631. [CrossRef]
24. Shen, X.; Li, B.; Hu, X.; Sun, C.F.; Hu, Y.S.; Yang, C.; Liu, H.; Zhao, J. Recycling Cathodes from Spent Lithium-Ion Batteries Based on the Selective Extraction of Lithium. *ACS Sustain. Chem. Eng.* **2021**, *9*, 10196–10204. [CrossRef]